Molecular Biology of the Cell
Vol. 13, 4470–4483, December 2002

Microtubule Asymmetry during Neutrophil Polarization and Migration

Robert J. Eddy, Lynda M. Pierini, and Frederick R. Maxfield*

Department of Biochemistry, Weill Medical College of Cornell University, New York, New York 10021

Submitted May 1, 2002; July 18, 2002; Accepted August 21, 2002
Monitoring Editor: Jennifer Lippincott-Schwartz

The development of cell polarity in response to chemoattractant stimulation in human polymorphonuclear neutrophils (PMNs) is characterized by the rapid conversion from round to polarized morphology with a leading lamellipod at the front and a uropod at the rear. During PMN polarization, the microtubule (MT) array undergoes a dramatic reorientation toward the uropod that is maintained during motility and does not require large-scale MT disassembly or cell adhesion to the substratum. MTs are excluded from the leading lamella during polarization and motility, but treatment with a myosin light chain kinase inhibitor (ML-7) or the actin-disrupting drug cytochalasin D causes an expansion of the MT array and penetration of MTs into the lamellipod. Depolymerization of the MT array before stimulation caused 10% of the cells to lose their polarity by extending two opposing lateral lamellipodia. These multipolar cells showed altered localization of a leading lamella-specific marker, talin, and a uropod-specific marker, CD44. In summary, these results indicate that F-actin– and myosin II-dependent forces lead to the development and maintenance of MT asymmetry that may act to reinforce cell polarity during PMN migration.

INTRODUCTION

Chemotaxis, the directed migration of leukocytes toward a source of chemoattractant, is a crucial step in the host immune response to infection. Circulating leukocytes respond to specific chemical signals generated at the site of inflammation by developing a polarized morphology with the formation of a lamellipodium at the leading edge and a uropod at the trailing edge. During cell polarization, the rapid nucleation and polymerization of actin at the leading edge drive the protrusion of the cell membrane, forming the leading lamellipodium. Further extension of the lamellipod is brought about by adhesion to the substratum via integrins and remodeling of the F-actin network, whereas cell retraction, driven by myosin II-generated forces, results in detachment of the uropod from the substratum. The temporal and spatial coordination of lamellar protrusion and uropod retraction is essential for efficient cell motility in response to chemotactic stimuli (Bretscher, 1996a; Lauffenburger and Horwitz, 1996; Mitchison and Cramer, 1996).

Although the requirement for actin polymerization in lamellar protrusion is absolute, the mechanisms by which a highly motile cell like the human polymorphonuclear neutrophil (PMN) maintains its polarity once it has been established are less well understood. Recent studies on PMN polarization have implicated myosin II-generated forces in the development and maintenance of cell polarity. Chemoattractant stimulation with *N*-formyl-L-methionyl-L-leucyl-L-phenylalanine (fMLF) in the presence of inhibitors of myosin II activation permitted cell spreading but prevented polarization, resulting in a broad lamellipodium around the cell perimeter (Eddy *et al.*, 2000). Furthermore, myosin II-generated forces also contribute to the rearrangement of large-scale, detergent-resistant membrane domains to the uropod after PMN polarization, perhaps serving to partition key molecules essential for the specific functions of the lamellipod and uropod (Seveau *et al.*, 2001).

To date, the role of the microtubule (MT) cytoskeleton during cell polarization and motility of PMNs upon chemoattractant stimulation remains uncertain. Many previous investigations probing the function of MTs in migrating PMNs have been hampered because conventional fixation protocols for immunofluorescence inadequately preserved the MT array (Ding *et al.*, 1995). Ultrastructural analysis of the orientation of the MT organizing center (MTOC) and MTs in PMNs undergoing chemotaxis were also limited by the inability to visualize the entire MT array (Malech *et al.*, 1977).

In addition, studies aimed at determining a role for MTs during cell migration through the use of specific inhibitors of MT polymerization have yielded conflicting results. Colchicine and nocodazole have been reported to stimulate random migration of PMNs (Stevenson *et al.*, 1978; Rich and

Article published online ahead of print. Mol. Biol. Cell 10.1091/mbc.E02–04–0241. Article and publication date are at www.molbiolcell.org/cgi/doi/10.1091/mbc.E02–04–0241.

* Corresponding author. E-mail address: frmaxfie@med.cornell.edu.

Hoffstein, 1981) or have no effect on random migration (Bandmann *et al.*, 1974; Lomnitzer *et al.*, 1976) or slightly inhibit random migration at high concentrations of drug (Ramsey and Harris, 1973). Related studies addressing the role of MTs during chemotaxis by treatment with these drugs have been equally conflicting with either impairment (Edelson and Fudenberg, 1973; Bandmann *et al.*, 1974) or no significant effect on cell orientation toward a chemoattractant source (Zigmond, 1977; Zigmond *et al.*, 1981). The issue is further complicated by the fact that MT-inhibiting drugs such as nocodazole trigger an F-actin–dependent cell polarization in PMNs in the absence of chemoattractant (Keller *et al.*, 1984).

Using a fixation and extraction protocol developed to maximize the preservation of PMN MTs for immunofluorescence (Ding *et al.*, 1995), we undertook a series of experiments designed to determine the role of MTs during PMN polarization and migration. After the initiation of cell polarization by the chemotactic peptide fMLF, the PMN MT network underwent a dramatic rearrangement, with the majority of individual MTs oriented toward the uropod and excluded from the F-actin–rich lamellipod. Furthermore, the development of an asymmetric MT array subsequent to PMN polarization was dependent on an intact actin cytoskeleton and activated myosin II. Disruption of the MT array resulted in defects in cellular polarity characterized by the extension of multiple leading lamellae in ~10% of the PMNs examined. In addition, alteration in the pattern of two polarity-specific markers, talin and CD44, was observed in MT-free PMNs. Evidence presented in this report supports a role for the asymmetric array of MTs in the reinforcement and maintenance of PMN polarity during cell migration.

MATERIALS AND METHODS

Reagents

Purified human fibronectin and vitronectin were purchased from Collaborative Research (Bedford, MA). ML-7 and ML-9 were purchased from Alexis (San Diego, CA). A rabbit polyclonal nonmuscle myosin II antibody was purchased from Biomedical Technologies (Stroughton, MA). A rabbit polyclonal peptide antibody (G2) specific for the γ isoform of nonmuscle actin was a generous gift from J.C. Bulinski (Columbia University, New York, NY). Anti-human CD44 mAb was purified from the Hermes-3 hybridoma (American Type Culture Collection, Manassas, VA). Alexa 546-conjugated phalloidin, Alexa 488, 546-conjugated goat anti-rabbit IgG (H+L), Alexa 546-conjugated goat anti-mouse IgG (H+L) were purchased from Molecular Probes (Eugene, OR). A mouse α-tubulin mAb (clone DM 1A) was purchased from Accurate Chemical (Westbury, NY). fMLF, cytochalasin D, nocodazole, saponin, taxol (paclitaxel), and purified human IgG were purchased from Sigma-Aldrich (St. Louis, MO).

PMN Isolation

Human PMNs were isolated from whole blood donated by healthy volunteers by a single-step separation over a Ficoll-Hypaque solution (Polymorphoprep) (Axis-Shield PoC, Oslo, Norway). Contaminating erythrocytes were lysed by a 30-s hypotonic shock in H_2O and the osmolarity of the medium was equilibrated by addition of 5× phosphate-buffered saline (PBS). Cells were then rinsed with PBS, resuspended in incubation buffer (150 mM NaCl, 5 mM KCl, 1 mM $MgCl_2$, 1 mM $CaCl_2$, 10 mM glucose, 20 mM HEPES, pH 7.4), and maintained at 22°C with gentle rotation to prevent cell aggregation.

Cytoskeletal Inhibitor Studies

For actin and myosin II inhibitor studies, ~1×10^5 PMNs were plated for 5 min at 37°C onto the coverslip area of an experimental chamber coated with 100 μg/ml human fibronectin in PBS. Cells were then treated with incubation medium containing the myosin light chain kinase (MLCK) inhibitors ML-7 [1-(5-iodonaphthalene-1-sulfonyl)-1*H*-hexahydro-1,4-diazepine, HCl] or ML-9 [1-(5-chloronaphthalenesulfonyl)-1*H*-hexahydro-1,4-diazepine, HCl] (10 or 35 μM, respectively) or the F-actin–disrupting drug cytochalasin D (1 μM). A bath application of 10 nM fMLF in incubation medium plus cytoskeletal inhibitors was added for the indicated times. For MT disruption studies, PMNs were plated at 37°C for 5 min, chilled on ice for 10 min, and then stimulated with 10 nM fMLF plus 10 μM nocodazole in incubation buffer at 37°C for the indicated times. To stabilize MTs, PMNs were plated as described, preincubated with 1 μM taxol (paclitaxel) for 30 min or 1 h at 37°C, and stimulated with 10 nM fMLF for the indicated times.

Cell Migration Assays

For MT disruption studies, cells were plated on fibronectin-coated coverslip chambers, chilled on ice for 10 min, stimulated with fMLF in the presence of nocodazole at 37°C, and immediately placed on a DMIRB microscope stage (Leica Microscopie and System), equipped with a cooled charge-coupled device camera (Micromax 512BFT; Princeton Scientific Instruments, Monmouth Junction, NJ) driven by Image-1/MetaMorph Imaging software (Universal Imaging, West Chester, PA). The microscope stage was maintained at 37°C by air curtain, and cell motility was monitored by taking single-frame images recorded every 20 s for a period of 4 min. MT disruption motility assays were repeated with three or more preparations of PMNs from different donors.

Immunofluorescence Microscopy

For optimized preservation of the PMN MT cytoskeleton, substrate-attached or suspended cells were prepared for immunofluorescence as described previously (Ding *et al.*, 1995). Briefly, cells were fixed in 0.7% glutaraldehyde in PBS, pH 7.4, and extracted with 0.5% Triton X-100 and 0.5% SDS for 15 min each. Autofluorescence was then quenched with 1 mg/ml $NaBH_4$ in PBS. For all other antigens, cells were fixed with 6.6% paraformaldehyde, 0.05% glutaraldehyde, 0.25 mg/ml saponin in PBS for 5 min. Nonspecific binding to F_c receptors was blocked for 30 min with PBS containing 10% heat-inactivated fetal calf serum, 0.25 mg/ml saponin (blocking buffer). For visualization of MTs, cells were stained with mouse α-tubulin mAb (clone DM 1A). Because the fixation procedure is incompatible with binding of the F-actin probe, phalloidin, the actin cytoskeleton was visualized using a polyclonal γ-actin antibody. This antibody has been shown to identify all actin-containing structures in cultured cells (Otey *et al.*, 1986) as well as PMNs (our unpublished observations). Cells were incubated with primary antibody for 1 h, washed extensively in blocking buffer, and incubated with the appropriate secondary antibody for 1 h at 1:200 dilution. To reduce nonspecific binding, all secondary antibodies were preabsorbed to fixed and F_c receptor-blocked PMNs in suspension for 2 h. All antibody incubations were performed at 22°C.

PMNs prepared for immunofluorescence were analyzed by confocal microscopy by using an LSM 510 laser scanning unit and an Axiovert 100 M inverted microscope equipped with a 63× 1.4 numerical aperture plan Apochromat objective (Carl Zeiss, Jena, Germany). Excitation on the LSM 510 unit was with a 25-mW argon laser emitting at 488 nm and a 1.0-mW helium/neon laser emitting at 543 nm, and emissions were collected using a 505- to 530-nm band pass filter to collect Alexa 488 emissions and a 585-nm-long pass filter to collect Alexa 546 emissions. In all images, a 0.4-μm vertical step size was used with a vertical optical resolution of <1.0 μm. Where otherwise indicated, all images are presented as summation projections of optical slices collected. All image processing,

quantification, analysis, and recording were performed with Image-1/MetaMorph Imaging software (Universal Imaging). To determine the distribution, length, and number of the MT array in PMNs, the paths of anti-α-tubulin (DM1A)-labeled filaments were manually traced from summation projections of confocal images and quantified using MetaMorph Imaging software. All images were printed using Adobe Photoshop 5.0 (Adobe Systems, Mountain View, CA) and a Spectra-Star DSx printer (General Parametrics, Berkeley, CA).

RESULTS

Polarized PMNs Display an Asymmetric MT Organization

We examined the MT array during chemoattractant-induced PMN polarity and motility by confocal microscopy with a protocol specifically designed to reliably preserve and label the MT cytoskeleton in human PMNs (Ding *et al.*, 1995). Changes in the spatial organization of the MT array during various stages of cell motility were investigated by plating cells on glass coverslips coated with fibronectin, a highly adhesive, physiologically relevant extracellular matrix protein. Random cell migration (chemokinesis) was then induced by a bath application of a chemoattractant, fMLF, at 10 nM. In our random migration assay, typically 85–90% of the cells become highly polarized and exhibit motility rates of 10–15 μm/min during the first 4 min after the addition of fMLF. At various times after fMLF stimulation, the cells were fixed and prepared for immunofluorescence as described in MATERIALS AND METHODS. The MT network was stained using a mAb directed against α-tubulin (DM1A) (Blose *et al.*, 1984) and costained with a polyclonal γ-actin antibody (Otey *et al.*, 1986) to visualize the actin cytoskeleton. Unstimulated PMNs plated on fibronectin-coated substratum are round and exhibit a delicate radial array of MTs emanating from a centrally located MTOC (Figure 1, A–F). Within 2 min after fMLF stimulation, PMNs become fully polarized with a distinct leading edge (lamellipod) and tail (uropod) and an MTOC located just behind the F-actin–containing lamella (Figure 1, G and J). The distribution of the MT array was quantified by manually tracing the paths of anti-tubulin–labeled filaments that emanated from the MTOC in each polarized cell. With an average of 22 microtubule filaments observed per cell, a consistent asymmetrical distribution of MTs was observed, with 84 ± 1% (n = 17 cells) of individual MTs oriented away from the leading lamella and toward the uropod (Figure 1, H and K). Similar asymmetric MT arrays were observed in PMNs crawling on another adhesive extracellular matrix protein, vitronectin (our unpublished data). Intense actin staining was found primarily at the leading lamellipod, opposite to the MT array (Figure 1, I and L). This asymmetric MT distribution persisted at 4 min after fMLF stimulation with 89 ± 1% (n = 11 cells) of MTs oriented toward the uropod (Figure 1, N and Q). Analysis of orthogonal projections of confocal sections demonstrate that the uropod-oriented MT array is not limited to the adherent lower surface but fills the entire volume of the cell body and uropod (our unpublished data). The polarization of MTs was readily reversible, because removal of the chemoattractant stimulus caused a rapid cell depolarization and return to a radial distribution of MTs (data not shown).

To test whether integrin engagement of extracellular matrix proteins is required for the asymmetric distribution of MTs, PMNs in suspension were stimulated with fMLF. PMNs stimulated in suspension are able to polarize, but the development of a distinct lamellipod and uropod occurs more slowly than in cells stimulated on fibronectin. Four minutes after fMLF stimulation, the emerging leading lamellipod, identified by its membrane ruffling and accumulation of F-actin, is localized to one pole (Figure 2, A–F), whereas the MT array begins to show clear orientation toward the uropod, opposite the emerging pseudopod. By 8 min poststimulation (Figure 2, G–L), the cells are well polarized with a distinct actin-rich leading lamellipod and uropod. As observed in PMNs polarized on fibronectin-coated substrates (Figure 1), cells polarized in suspension display a highly asymmetric distribution of MTs toward the uropod, with few if any MTs oriented toward the leading lamellipod.

Polarization of MTs Does Not Require Localized MT Disassembly

During the initial phase of PMN polarization, a rapid reorientation of the MT cytoskeleton from a radial array to a uropod-directed array is observed within 1 min after fMLF stimulation. One mechanism that could give rise to this asymmetry would be a localized disassembly of the MT network in the vicinity of the expanding lamellipod, whereas MTs in the forming uropod are retained. To test this possibility, we preincubated PMNs with the MT stabilizing drug taxol to prevent depolymerization and analyzed the MT array at various times after stimulation. Treatment with 1 μM taxol for 30 min before stimulation was sufficient to stabilize PMN MTs without excessive bundling and had no significant effect on cell polarization or random migration. At either 2 or 4 min after fMLF stimulation, no evidence of an increased retention of MTs in the vicinity of the leading lamella was in the taxol-treated cells (Figure 3). Furthermore, taxol-stabilized MTs became oriented toward the uropod at 2 and 4 min poststimulation in a similar manner to that of control cells.

Role of Actin in Exclusion of MTs from Leading Lamella

During chemotaxis, the establishment of cell polarity in many highly motile cells, including PMNs, is characterized by extensive ruffling and lamellipod extension at the leading edge. This ruffling and forward protrusion is dependent on the rapid polymerization and cross-linking of an actin meshwork. A mechanism that could contribute to development of MT asymmetry would be the exclusion of MTs by the expanding lamellipod. To test this idea in the absence of cell polarization, we used a "frustrated phagocytosis" assay in which PMNs were plated on a glass coverslip coated with purified, nonimmune human IgG. The cells develop a flattened, "fried egg" morphology with a broad, F-actin–rich lamellipod around the perimeter of cell. Analysis of the MT cytoskeleton in these cells clearly demonstrates a restriction of the MT array to the central cell body with few if any MTs penetrating the F-actin–containing radial lamella or contacting the cell membrane (Figure 4, A–F).

To test the role of actin polymerization in the exclusion of MTs by the leading lamella, cells were treated with the actin-disrupting drug cytochalasin D. Preincubation of PMNs for 5 min with 1 μM cytochalasin D followed by fMLF

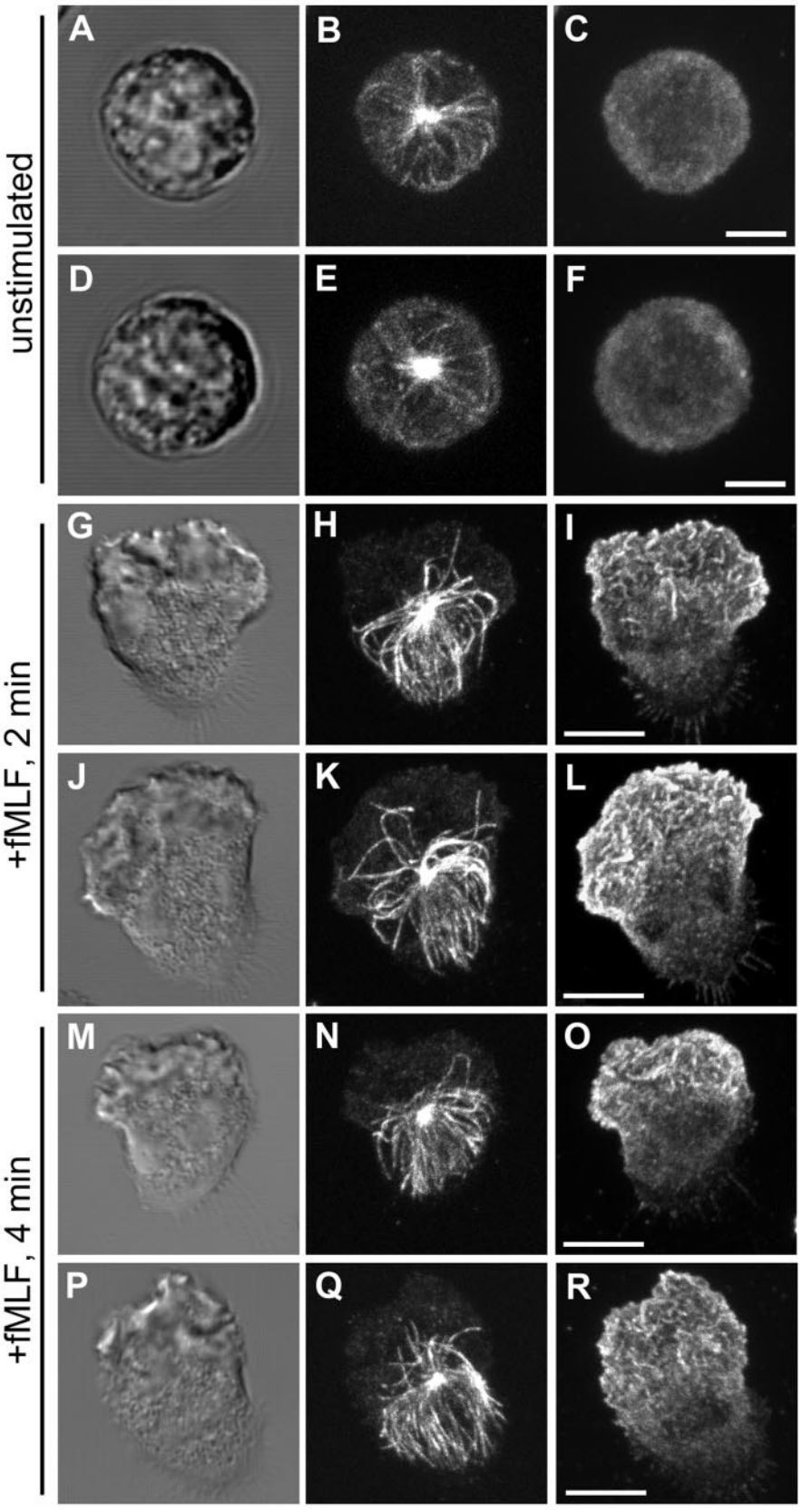

Figure 1. MTs reorient toward the uropod after polarization by fMLF on fibronectin (Fn)-coated surfaces. PMNs were plated on Fn-coated coverslips and stimulated with 10 nM fMLF for various times before fixation, and prepared for immunofluorescence as described in the MATERIALS AND METHODS. The MT array (B, E, H, K, N, and Q) and actin cytoskeleton (C, F, I, L, O, and R) were visualized by confocal microscopy. Differential interference contrast image (A, D, G, J, M, and P). Fluorescent images represent Z-axis confocal projections. Unstimulated (A–F), 2 min after fMLF stimulation (G–L), and 4 min after fMLF stimulation (M–R). Bar, 5 μm.

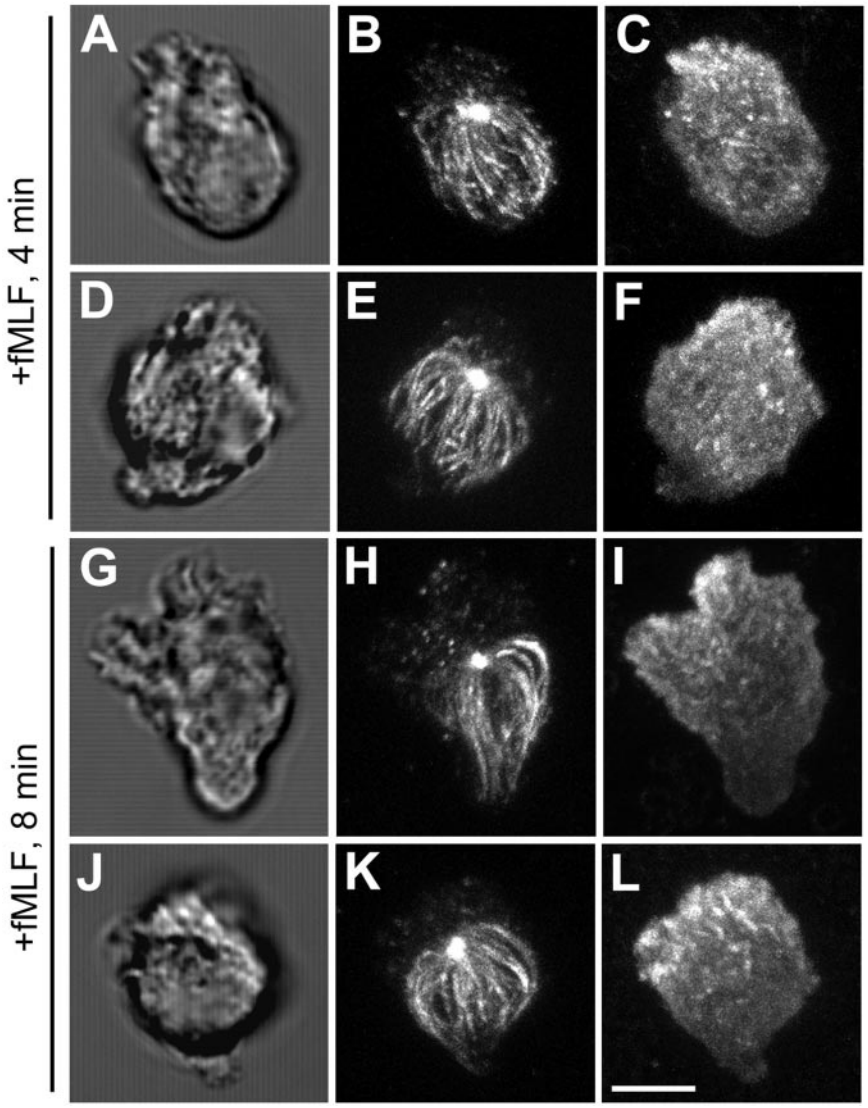

Figure 2. MTs reorient toward the uropod after polarization by fMLF in suspended cells. Suspended PMNs in the absence of extracellular matrix coated substrate were stimulated with 10 nM fMLF for various times before fixation. The MT array (B, E, H, and K) and actin cytoskeleton (C, F, I, and L) were visualized by confocal microscopy. Differential interference contrast image (A, D, G, and J). Fluorescent images represent Z-axis confocal projections. Four minutes after fMLF stimulation (A–F) and 8 min after fMLF stimulation (G–L). Bar, 5 μm.

stimulation in the presence of cytochalasin D blocked cell polarization and produced a round, but highly flattened cell morphology (Figure 4, G–L). Diffuse actin staining was found throughout the cytoplasm and in a thin layer just beneath the cell membrane, in agreement with previous observations (Pryzwansky and Merricks, 1998). The majority of individual MTs in cytochalasin D-treated PMNs emerged from the MTOC in a radial pattern and extended out to the cell periphery. MTs were often found in close apposition with the cell membrane for several microns or looped backwards after making contact with the membrane. As a consequence of disassembly of the actin cytoskeleton by cytochalasin D, we observed an overall enhancement in the MT array. The MT array was quantified by manually tracing the paths of anti-tubulin–labeled filaments that emanated from the MTOC in cells under control and experimental conditions. An approximate 2.1-fold increase in MT length and 1.4-fold increase in the number of MTs per cell was observed in cytochalasin D-treated cells compared with control cells (Table 1), suggesting the actin cytoskeleton plays an active role in the orientation of the MT array.

Role of Myosin II in Development of MT Asymmetry during Polarization

We have previously demonstrated that activated myosin II is localized to the uropod as well as the leading lamella in motile PMNs crawling on adhesive surfaces such as fibronectin. Disruption of myosin II function by using the MLCK inhibitors ML-7 and ML-9 blocks cell polarization and induces the formation of a band of F-actin around the perimeter of the cell (Eddy *et al.*, 2000). These results suggest that myosin II activation is required for the proper formation and maintenance of a polarized lamellipodia.

To test whether myosin II activation is involved in development of MT asymmetry in polarizing PMNs, cells were treated the MLCK inhibitor ML-7. Preincubation of cells with 10 μM ML-7, followed by fMLF stimulation in the

Table 1. Quantification of change in the microtubule array following cytochalasin D and ML-7 treatment

	MT length (μm)	MT number	(n)
Control	5.75 ± 0.08	22.14 ± 0.14	278
Cytochalasin D	11.67 ± 0.17	30.19 ± 0.28	171
ML-7	11.99 ± 0.16	30.62 ± 0.4	237

The MT array in PMNs was quantified by manually tracing the paths of anti-α-tubulin labeled filaments from confocal images. Data represent average number and length (μm) ± SEM of individual microtubules from 18 control, 11 cytochalasin D-treated (Fig. 4), and 11 ML-7-treated cells (Fig. 5) from two independent experiments. (n), the number of individual microtubules analyzed for each condition.

presence of ML-7, blocked both cell motility and polarization and produced a round, highly flattened cell morphology (Figure 5, A–F). The majority of individual MTs emerged from the MTOC in a radial pattern, in close apposition with the cell membrane in a similar manner to PMNs stimulated with fMLF in the presence of cytochalasin D. MLCK inhibition also caused an enhancement of the MT array with an approximate 2.1-fold increase in MT length and 1.4-fold increase in the number of MTs per cell compared with control cells (Table 1). Similar results were obtained using 35 μM ML-9, a chemically related MLCK inhibitor (our unpublished data). The magnitude of increase in both MT length and number in the presence of ML-7 was indistinguishable from that observed in cells stimulated with fMLF in the presence of cytochalasin D.

On washout of ML-7 in the continued presence of fMLF, cells can rapidly undergo polarization and resume normal motility (Eddy *et al.*, 2000). To confirm a role for myosin II activation in the development of MT asymmetry during polarization, we analyzed changes in the distribution of the MT array in cells released from ML-7 inhibition. Cells were preincubated with 10 μM ML-7 for 5 min and then stimulated with fMLF in the presence of 10 μM ML-7 for 4 min. The ML-7 was then removed in the continued presence of fMLF, and the MT array was analyzed at various times after ML-7 washout (Figure 5, G–X). Within 1 min after ML-7 washout, a nascent lamellipod, identified by its accumulation of actin, is visible at one pole of the cell. Meanwhile, the MT array is beginning to show signs of orientation toward the opposite pole. By 2 min after ML-7 washout, reorientation of the MT array toward the forming uropod is readily discernible. Most strikingly, we observe individual MTs which extend toward the leading lamella assume a bent or looped configuration (Figure 5, N and Q). After 5 min, a pronounced orientation of the MT array toward the uropod was observed with few MTs in the vicinity of the leading lamella (Figure 5, S–X).

Free MT Fragments Are Found at Leading Lamella during Cell Polarization and Motility

During our observations of the MT array in polarizing PMNs, short fragments of MTs between 0.5 and 1 μm in length were detected in the vicinity of the leading lamellipod. Confocal analysis of 0.4-μm optical sections determined that these fragments were free and not associated with the MTOC (Figure 6). MT fragments in the leading lamella were observed at 2 min after washout from ML-7 (Figure 6B) as well as 2 min after fMLF stimulation (Figure 6E). At either 4 min after ML-7 washout or fMLF stimulation, the presence of fragments in the vicinity of the leading lamella was more infrequent, suggesting the generation of these fragments is a transient phenomena associated with the establishment of polarity. In addition, we observed a significant increase in the number of these fragments in cells pretreated with 1 μM taxol (Figure 3B).

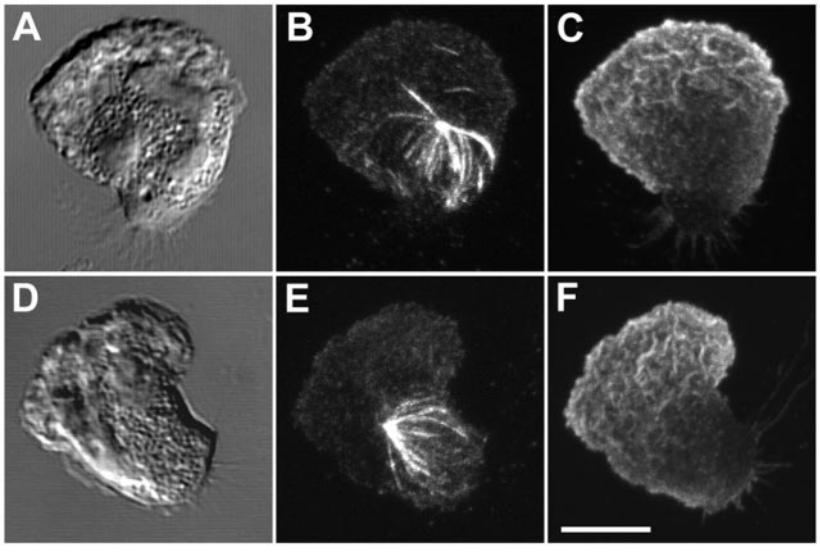

Figure 3. Reorientation of the MT array in the presence of taxol. PMNs were plated on fibronectin (Fn)-coated coverslips, preincubated with 1 μM taxol for 30 min, and stimulated with 10 nM fMLF for various times. The MT array (B and E) and actin cytoskeleton (C and F) were visualized by confocal microscopy. Differential interference contrast image (A and D). Fluorescent images represent Z-axis confocal projections 2 min after fMLF stimulation (A–C) or 4 min after fMLF stimulation (D–F). Bar, 5 μm.

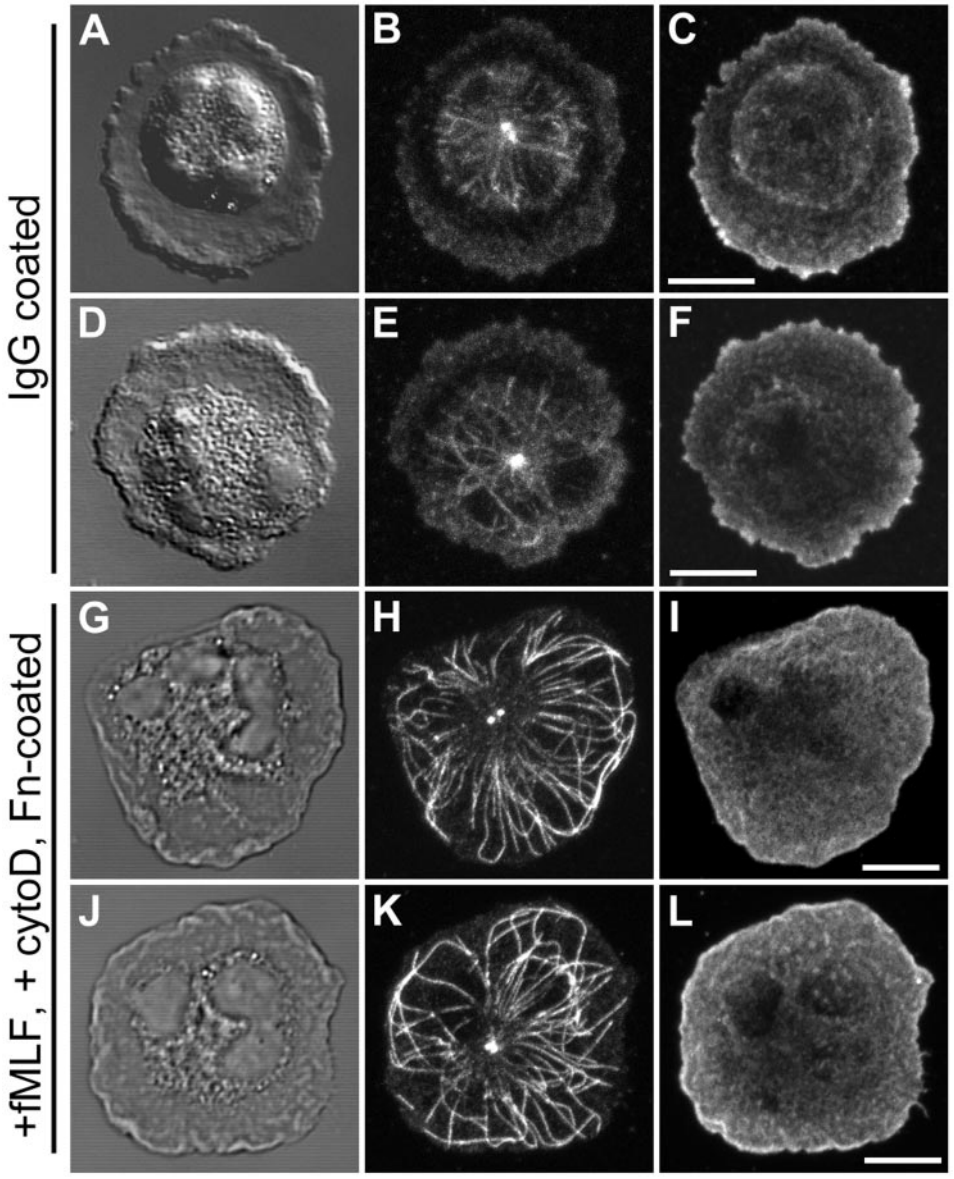

Figure 4. Role of actin cytoskeleton in MT asymmetry. (A–F) Pattern of the MT array during "frustrated phagocytosis". PMNs were plated on human nonimmune IgG for 4 min before fixation. (G–L) Pattern of the MT array after F-actin disruption. PMNs were plated on fibronectin (Fn)-coated coverslips, preincubated with 1 μM cytochalasin D for 4 min and stimulated with 10 nM fMLF plus cytochalasin D for 4 min before fixation. The MT array (B, E, H, and K) and actin cytoskeleton (C, F, I, and L) were visualized by confocal microscopy. Differential interference contrast image (A, D, G, and J). Fluorescent images represent Z-axis confocal projections. Bar, 5 μm.

MT Depolymerization Leads to Defects in Maintenance of Cell Polarity

The use of MT inhibitors such as nocodazole, colchicines, or vinblastine to investigate the role of MTs during PMN polarization is problematic. Although cell polarization can be achieved by 1 min after fMLF stimulation, MT inhibitors such as nocodazole require at least 5 min to achieve nearly complete disassembly of MTs in PMNs as evaluated by an optimized immunofluorescence protocol (Ding *et al.*, 1995). To overcome the limitations of these drugs, PMNs were first incubated on ice for 10 min, to ensure depolymerization of the preexisting MT array, and then stimulated with fMLF in the presence of 10 μM nocodazole at 37°C to prevent growth of any new MTs during cell polarization. Essentially, complete depolymerization of MTs was achieved using this protocol as confirmed by immunofluorescence staining for α-tubulin with DM1A (our unpublished data).

Alterations in cell polarization and motility on fibronectin-coated substrates of MT-free PMNs were monitored by time-lapse video microscopy over a 5-min period. Within 2 min after addition of fMLF plus nocodazole, a subpopulation of cells, averaging 10 $\pm$ 1% (n = 1401 cells) seemed to cease normal random motility and extend two lamellipodia in opposite directions from the original leading lamella. The two lateral lamellipodia remained connected by a cytoplasmic "bridge" region that varied in length from 5 to 15 μm. At 4 min poststimulation, an average of 7 $\pm$ 0.5% (n = 1470 cells) of the total cells exhibited this multipolar morphology. There was no significant change in the number of unpolarized cells at either 2 or 4 min

poststimulation compared with control, demonstrating that the MT depolymerization protocol had no negative affect on cell viability. Two distinct outcomes were observed during analysis of MT-free PMNs exhibiting two leading lamella. One outcome, shown in Figure 7, is that one leading lamella becomes the dominant lamellipod, whereas the secondary lamellipod is retracted into the cell. After establishment of a dominant lamellipod, the cell often resumed normal motility. However, in some cases, the two lamellipodia continued to extend in opposite directions, as if the cell were attempting to undergo cytokinesis. In these cases, the cell did not resolve into a single, dominant leading lamellipodia but instead remained locked in this multipolar morphology for up to 10 min of observation.

In the remainder of the MT-free cells that did not exhibit this polarity defect, cell polarization and rates of motility were similar to control cells in agreement with previous studies (Keller *et al.*, 1984), although increased frequency of turning was noted, confirming previous observations (Allan and Wilkinson, 1978).

Distribution of Polarity-specific Markers in Multipolar Cells Lacking MTs

Numerous membrane receptors, adhesion molecules, and cytoskeletal proteins undergo a change in their cellular distribution upon cell polarization (Sanchez-Madrid and del Pozo, 1999). For example, the leading lamellipod can be identified by the accumulation of F-actin as well as focal adhesion-associated proteins such as talin (Eddy *et al.*, 2000). Proteins that redistribute to the uropod upon cell polarization include membrane receptors such as CD43 and CD44 (Seveau *et al.*, 1997, 2001). To further characterize the multipolar cell morphology, we examined the distribution of these lamellipod- or uropod-specific markers in cells devoid of MTs. Talin and F-actin were colocalized primarily at the edges of both opposing lamellipodia (Figure 8, A–F). Often, talin and F-actin staining were more pronounced in one of the lamellipodia compared with the other. The talin-poor lamellipodia may have been undergoing retraction rather than expansion, because they typically did not accumulate large amounts of F-actin and lacked ruffles or filopodia. F-actin, but not talin, was also found in the bridge region of the cell that linked the two opposing lamellipodia. The uropod-specific marker CD44 was somewhat concentrated in the bridge region and colocalized with F-actin (Figure 8, G–L).

DISCUSSION

After chemoattractant stimulation, a distinctive polarity is rapidly established within the PMN coinciding with the emergence of a highly ruffled leading lamella at the front and a tapered uropod at the rear. Our study has revealed a reorientation of the MT array during cell polarization and migration. Unstimulated cells possess an isotropic MT configuration that becomes reoriented toward the forming uropod within 2 min after chemotactic stimulation with fMLF. This striking asymmetry in the MT array persisted as long as the cell remained polarized and was observed in cells stimulated in suspension, showing that substrate attachment through integrin receptors is not required to reorient the MT array toward the uropod.

Our observation of a uropod-directed MT array in motile PMNs has distinct differences compared with slower moving cells. For example, 3T3 fibroblasts induced to migrate after wounding of a cell monolayer exhibit an asymmetric, stable MT array consisting of Glu-tubulin oriented toward the leading edge (Gundersen and Bulinski, 1988). It seems that development of an asymmetric MT array often accompanies cell polarization, but differences in the reorientation of the array may be cell-type specific or depend on the relative speed at which the cell migrates.

Mechanisms for Generating MT Asymmetry

The reorientation from an isotropic MT array to an asymmetric array upon cell polarization could arise through several possible mechanisms. During the initial stages of cell polarization, a uropod directed array could result from either 1) a partial disassembly of the randomly oriented array in the front half of the polarizing cell while the MTs in the uropod remain intact, or 2) a rapid retraction of the entire preexisting random array toward the uropod. We found that uropod reorientation of the MT array occurred in the PMNs preincubated with taxol before stimulation, effectively ruling out a mechanism requiring disassembly or large-scale remodeling of the array. These results are in agreement with previous observations of reorientation of taxol-treated MT arrays toward the uropod in migrating T cells (Ratner *et al.*, 1997).

One hallmark of cell polarization is the localized polymerization of actin at one side of the cell, giving rise to the leading lamellipod. Highly motile cells such as PMNs expand and maintain the leading lamella through intrinsic cycles of actin nucleation and polymerization, actin filament cross-linking into an orthogonal network, and subsequent remodeling of the actin network. We have previously found that activated myosin II, an F-actin motor, is localized to the leading lamella in motile PMNs, and blocking myosin II function by MLCK inhibition prevents cell polarization and causes the cell to extend a radial lamellipod in response to fMLF. This indicates that contractile forces generated by myosin II are necessary for extension of a polarized lamellipod (Eddy *et al.*, 2000). With this in mind, we postulated that forces exerted by actin and myosin II in the extending lamella might play a role in MT asymmetry during polarization by excluding MTs from this region. This hypothesis is supported by previous studies that found an exclusion of in vivo labeled MTs from the lamellipodia in migrating normal rat kidney fibroblasts (Mikhailov and Gundersen, 1998) as well as epithelial cells (Waterman-Storer and Salmon, 1997). In PMNs, we found that inhibiting actin polymerization by cytochalasin D or contractile force generation by inhibiting MLCK resulted in a highly flattened, nonpolar morphology and caused a significant increase in both MT length and number. Cytochalasin D or ML-7–treated cells did not exclude MTs from the lamellar F-actin network as evidenced by the numerous MTs extending to and along the membrane. Moreover, cells plated on IgG also maintain a highly flattened and nonpolar morphology but contain a relatively short MT array that is generally excluded from the broad F-actin–rich radial lamella, with very few MTs extending to the cell membrane. In cells released from ML-7 inhibition, the MT array rapidly reorients from an isotropic MT array to a uropod-directed one. In addition, MTs appeared looped or deflected away from the emerging lamellipod, reinforcing our premise that lamellipod expansion or actin myosin contractile forces within lamellae can exclude MTs in polarizing PMNs. The appearance of short fragments of MTs not associated with the

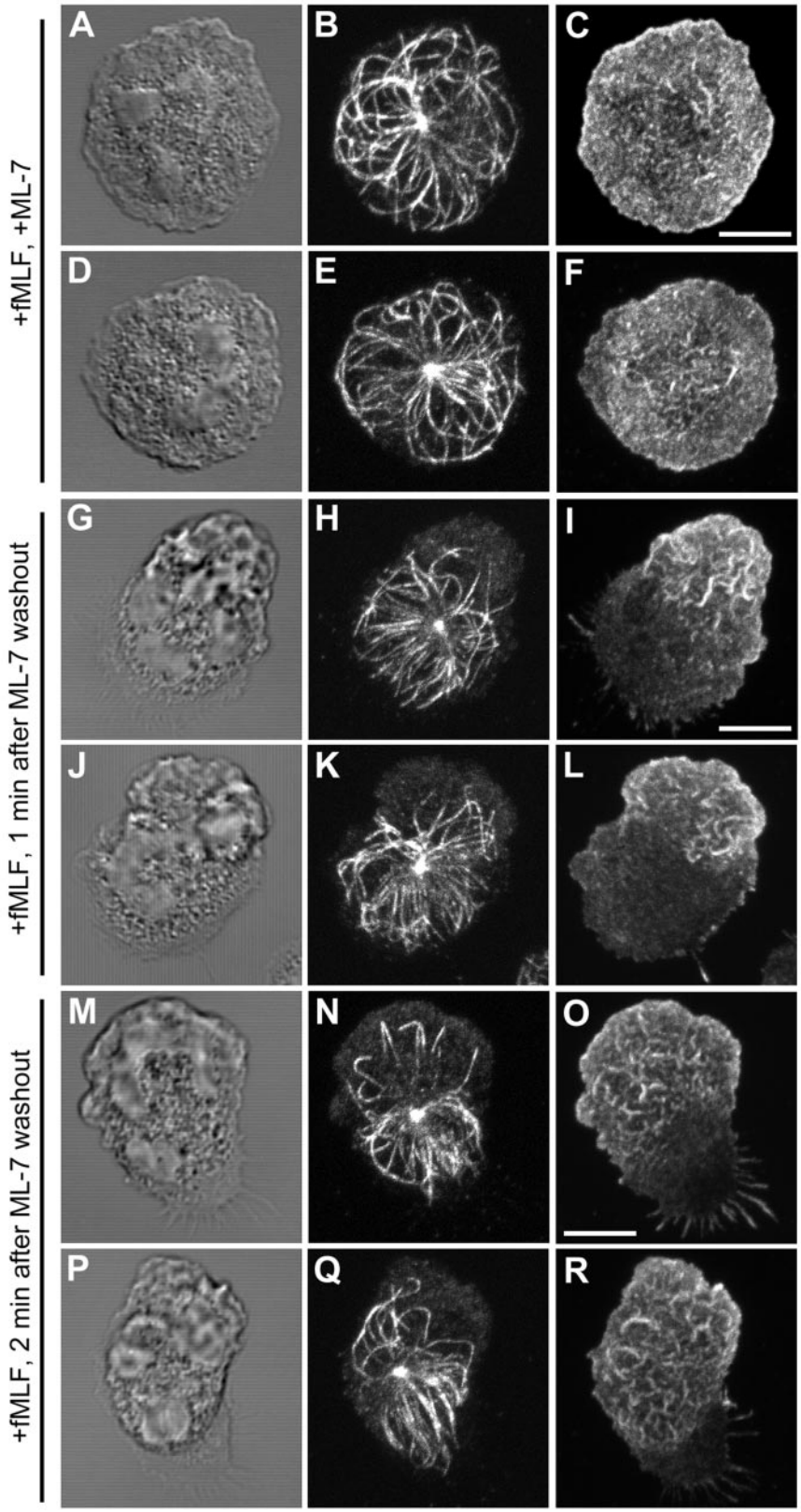
+fMLF, +ML-7
+fMLF, 1 min after ML-7 washout
+fMLF, 2 min after ML-7 washout
A
B
C
D
E
F
G
H
I
J
K
L
M
N
O
P
Q
R

Figure 5.

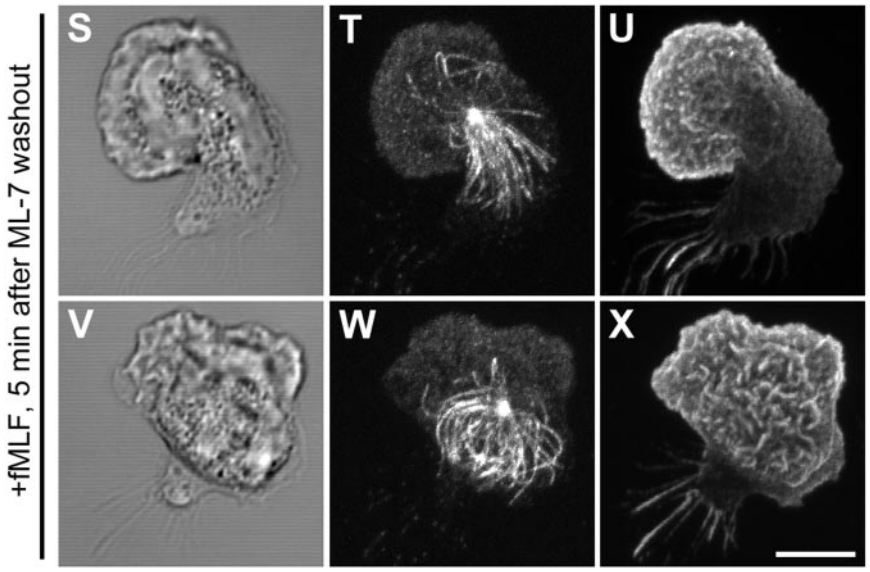

Figure 5 (cont). Role of myosin II activation in MT asymmetry. PMNs were plated on fibronectin (Fn)-coated coverslips, preincubated with 10 μM ML-7 for 5 min and stimulated with 10 nM fMLF plus ML-7 for 4 min before fixation. The MT array (B, E, H, K, N, Q, T, and W) and actin cytoskeleton (C, F, I, L, O, R, U, and X) were visualized by confocal microscopy. DIC image (A, D, G, J, M, P, S, and V). Fluorescent images represent Z-axis confocal projections. 4 min following fMLF stimulation in the presence of ML-7 (A-F); 1 min following ML-7 washout (G-L); 2 min following ML-7 washout (M-R), MTs near the leading lamella are looped or bent toward the uropod. At 5 min following ML-7 washout (S-X), the majority of MTs show a uropod orientation. Bar, 5 μm.

MTOC in the vicinity of the lamellipod within 2 min after fMLF stimulation or release from MLCK inhibition could result from fragmentation of the looped or bent MTs we observe (Figure 7B). This phenomena may be analogous to MTs positioned just behind the leading lamella in slower moving newt lung epithelial cells, which undergo buckling and breakage due to actomyosin-dependent retrograde flow (Waterman-Storer and Salmon, 1997). Therefore, it seems plausible that MT fragments generated in the leading lamellipod of PMNs could undergo dynamic instability and rapid disassembly, contributing to the maintenance of MT asym-

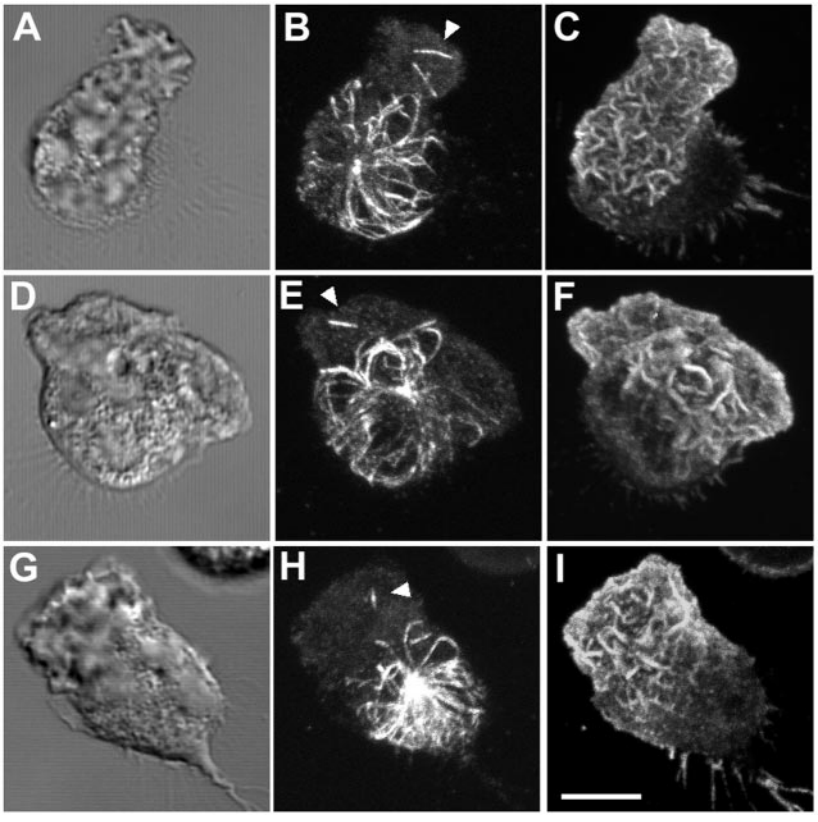

Figure 6. Presence of free MTs in the leading lamella of polarizing PMNs. The MT array (B, E, H) and actin cytoskeleton (C, F, I) were visualized by confocal microscopy. Differential interference contrast image (A, D, and G). Fluorescent images represent Z-axis confocal projections. In A–C, PMNs plated on fibronectin (Fn)-coated coverslips, were preincubated with 10 μM ML-7 for 5 min, stimulated with 10 nM fMLF plus ML-7 for 4 min. After washout of the ML-7, the cells were allowed to polarize for 2 min before fixation (A–C). In D–I, control PMNs were stimulated with fMLF for 2 min (D–F) and 4 min (G–I) before fixation. Free MTs not associated with the MTOC are indicated with an arrowhead. Bar, 5 μm.

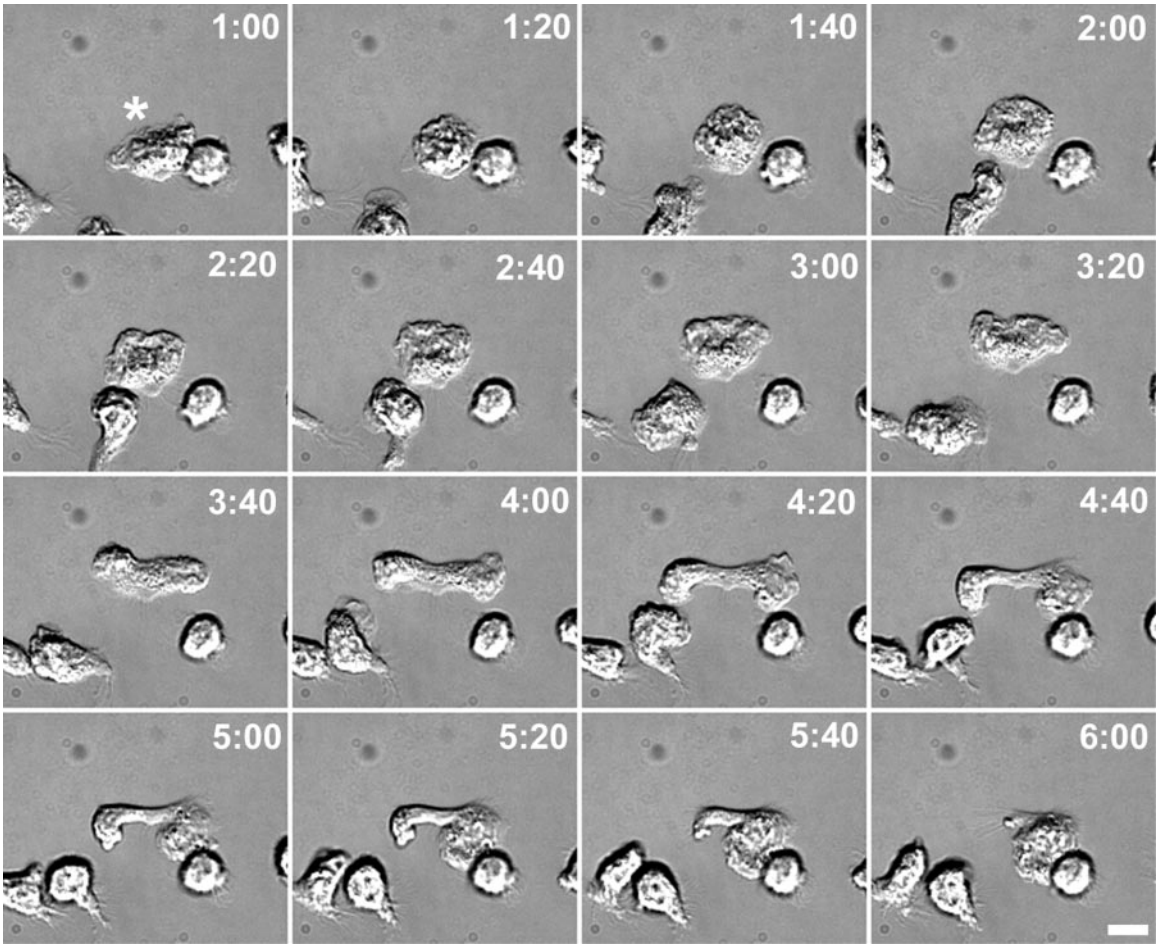

Figure 7. Defects in the maintenance of cell polarity in MT-free PMNs. PMNs were plated on fibronectin (Fn)-coated coverslips, incubated on ice for 10 min, and stimulated with 10 nM fMLF plus 10 μM nocodazole at 37°C, and differential interference contrast images were taken at various times indicated (minutes:seconds). The leading lamella is indicated by an asterisk. At 2:00 after fMLF stimulation, the cell stops migrating. Between 2:20 and 4:00, the cell extends two lateral lamellipodia, in opposite directions and parallel to the initial direction of motility. By 4:20, the lateral lamellipodia, connected by a membranous bridge, reach their maximum extension. At 5:00, the right lateral lamellipod becomes the new leading lamellipod, while the left lateral lamellipod retracts into the cell body. Bar, 5 μm.

metry as the cell migrates. Alternatively, the noncentrosomal MT fragments we observe in the vicinity of the leading lamella may form de novo as demonstrated in A498 kidney carcinoma cells (Yvon and Wadsworth, 1997). Until novel methods to study MT dynamics in living PMNs are developed, the question as to the origin of these MT fragments will remain speculation. Based on this evidence, it is likely that myosin II-based contractile forces generated within the F-actin network may contribute to the MT asymmetry by first reorienting the MT to the uropod during cell polarization and maintaining MT asymmetry during cell migration by excluding and/or fragmenting MTs in the vicinity of the leading lamella.

Role of Asymmetric MTs during Motility

What might be the function of the MT reorientation we observe in migrating PMNs? It has been proposed that in T cells, MT reorientation may overcome the negative effects of the MT array on motility (Ratner *et al.*, 1997). Because the relative rigidity of MTs limit cell deformability, retraction of the MT array into the uropod would "streamline" the cell and facilitate passage through narrow collagen matrices or endothelial monolayers (Ratner *et al.*, 1997). Our similar observations of MT reorientation on fibronectin-coated surfaces would support such a model. The uropod-directed MT array might also play a role in regulating uropod retraction during motility. Defects in uropod retraction and increased cell adhesion leading to decreased motility rates has been reported in PMA-stimulated B16 melanoma cells treated with nocodazole (Ballestrem *et al.*, 2000). In addition, repeated targeting of MTs to focal contacts have been proposed to deliver relaxing signals in fibroblasts, resulting in the release of focal contacts sites that would enable the cell to move forward (Kaverina *et al.*, 1999; Small *et al.*, 1999). However, uropod-directed MTs would most likely play a very minor role in PMN detachment from adhesion sites during random migration, because we saw no evidence of

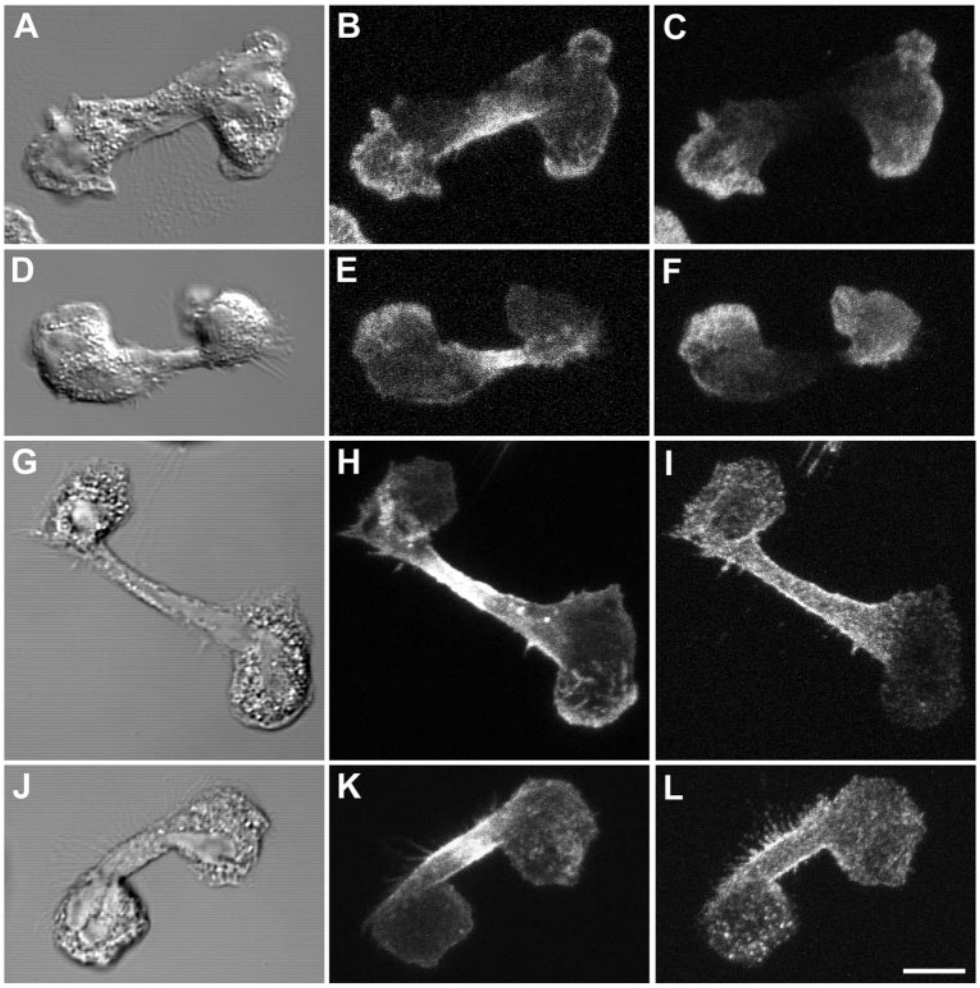

Figure 8. Talin and CD44 localization in MT-free multipolar cells. PMNs were plated on fibronectin (Fn)-coated coverslips, incubated on ice for 10 min and stimulated with 10 nM fMLF plus 10 μM nocodazole at 37°C for 2 min before fixation. Images were visualized by confocal microscopy. Differential interference contrast image (A, D, G, and J). Fluorescent images represent Z-axis confocal projections. F-actin (B, E, H, and K), talin (C and F), and CD44 (I and L). Bar, 5 μm.

defects in tail retraction nor increased adhesion to a variety of adhesive substrates in PMNs devoid of MTs.

The dramatic alterations in cell polarity and loss of random motility in the 10% of the MT-free cells that develop multiple leading lamellae suggests that the MT array is not entirely dispensable for PMN random migration after chemotactic stimulation as previous studies have concluded (Ramsey and Harris, 1973; Bandmann *et al.*, 1974; Lomnitzer *et al.*, 1976) and support previous observations with colcemid-treated guinea pig alveolar macrophages (Glasgow and Daniele, 1994). In light of our observations, we reasoned that the reorientation of the MT array to the uropod might act to reinforce PMN polarity once it has been established after stimulation.

How might the asymmetric MT array reinforce cell polarity during PMN migration? One possibility is that the MT array plays an important role in maintaining cell polarity by modulating the activity of Rho family GTPases, key regulators of actin dynamics and organization (Wittmann and Waterman-Storer, 2001). Another important function of MTs is to serve as tracks for the long-range movement of membrane vesicles (Vale, 1987). Motion analysis of PMNs that have endocytosed the fluorescent lipid analog C_6-NBD-GalCer has shown that as cells move, the endosomal recycling compartment (ERC) is localized just behind the leading lamellipod, and the ERC is reoriented rapidly as cells turn (Pierini *et al.*, 2000). The asymmetric MT array would cause recycling membrane to be brought from sites of endocytosis throughout the uropod to a position just behind the leading lamellipod. Because the proper positioning and organization of the ERC in polarized PMNs are dependent on an intact MT array (our unpublished data) as in other cell types (McGraw *et al.*, 1993), and cells devoid of MTs lost cell polarity by extending multiple lamellipodia nonvectorially (Figure 7), it is possible that the directed transport of vesicles to the ERC along MTs could play a role in the maintenance of PMN polarity.

We speculate that recycling of certain molecules, including integrins, might provide a link between the asymmetric MT distribution and maintenance of polarity. We have shown previously that $\alpha5\beta1$ and $\alpha v\beta3$ integrins in PMNs are endocytosed, and these integrins maintain a gradient of expression in the adherent membrane toward the front of migrating PMNs (Lawson and Maxfield, 1995; Pierini *et al.*, 2000). The $\alpha5\beta1$ integrin was shown to colocalize with other endocytic tracers in the ERC (Pierini *et al.*, 2000). Given the

low abundance of $\alpha5\beta1$ and $\alpha v\beta3$ integrins in these cells, it has not been possible to directly image the release of recycled integrins in living cells. However, indirect evidence indicates that integrins are released toward the front of migrating PMNs (Lawson and Maxfield, 1995; Pierini *et al*., 2000) but not in the leading lamella, which is free of membrane organelles (Boyles and Bainton, 1979). Further experiments, including direct observation of integrin recycling, will be necessary to test this hypothesis rigorously.

In summary, the data presented herein support a mechanism whereby small, rapidly motile cells such as the PMN establish and maintain cell polarity through an actin- and myosin II-dependent reorientation of the MT array toward the uropod. This reorientation could serve to "streamline" the cell by compacting the MT array into the uropod, thereby 1) facilitating polarization and maximizing cell motility on two- or three-dimensional matrices; and/or 2) providing positional information that would serve to reinforce cell polarity during migration, possibly through the directed endocytic recycling of vesicles toward the front of the cell.

ACKNOWLEDGMENTS

We thank Dr. Stephanie Seveau for the CD44 antisera and Dr. Robert Vasquez for comments and insight during the preparation of this manuscript. This work was supported by National Institutes of Health grant GM-34770 (to F.R.M.).

REFERENCES

Allan, R.B., and Wilkinson, P.C. (1978). A visual analysis of chemotactic and chemokinetic locomotion of human neutrophil leukocytes. Use of a new chemotaxis assay with *Candida albicans* as gradient source. Exp. Cell Res. *111*, 191–203.

Ballestrem, C., Wehrle-Haller, B., Hinz, B., and Imhof, B.A. (2000). Actin-dependent lamellipodia formation and microtubule-dependent tail retraction control directed cell migration. Mol. Biol. Cell *11*, 2999–3012.

Bandmann, U., Rydgren, L., and Norberg, B. (1974). The difference between random movement and chemotaxis. Effects of antitubulins on neutrophil granulocyte locomotion. Exp. Cell Res. *88*, 63–73.

Blose, S.H., Meltzer, D.I., and Feramisco, J.R. (1984). 10-nm filaments are induced to collapse in living cells microinjected with monoclonal and polyclonal antibodies against tubulin. J. Cell Biol. *98*, 847–858.

Boyles, J., and Bainton, D.F. (1979). Changing patterns of plasma membrane-associated filaments during the initial phases of polymorphonuclear leukocyte adherence. J. Cell Biol. *82*, 347–368.

Bretscher, M.S. (1996a). Getting membrane flow and the cytoskeleton to cooperate in moving cells. Cell. *87*, 601–606.

Ding, M., Robinson, J.M., Behrens, B.C., and Vandre, D.D. (1995). The microtubule cytoskeleton in human phagocytic leukocytes is a highly dynamic structure. Eur. J. Cell Biol. *66*, 234–245.

Eddy, R.J., Pierini, L.M., Matsumura, F., and Maxfield, F.R. (2000). Ca^{2+}-dependent myosin II activation is required for uropod retraction during neutrophil migration. J. Cell Sci. *113*, 1287–1298.

Edelson, P.J., and Fudenberg, H.F. (1973). Effect of vinblastine on the chemotactic responsiveness of normal human neutrophils. Infect. Immun. *8*, 127–129.

Glasgow, J.E., and Daniele, R.P. (1994). Role of microtubules in random cell migration: stabilization of cell polarity. Cell Motil. Cytoskeleton *27*, 88–96.

Gundersen, G.G., and Bulinski, J.C. (1988). Selective stabilization of microtubules oriented toward the direction of cell migration. Proc. Natl. Acad. Sci. USA *85*, 5946–5950.

Kaverina, I., Krylyshkina, O., and Small, J.V. (1999). Microtubule targeting of substrate contacts promotes their relaxation and dissociation. J. Cell Biol. *146*, 1033–1044.

Keller, H.U., Naef, A., and Zimmermann, A. (1984). Effects of colchicine, vinblastine and nocodazole on polarity, motility, chemotaxis and cAMP levels of human polymorphonuclear leukocytes. Exp. Cell Res. *153*, 173–185.

Lauffenburger, D.A., and Horwitz, A.F. (1996). Cell migration: a physically integrated molecular process. Cell *84*, 359–369.

Lawson, M.A., and Maxfield, F.R. (1995). Ca^{2+}- and calcineurin-dependent recycling of an integrin to the front of migrating neutrophils. Nature *377*, 75–79.

Lomnitzer, R., Rabson, A.R., and Koornhof, H.J. (1976). Leukocyte capillary migration: an adherence dependent phenomenon. Clin. Exp. Immunol. *25*, 303–310.

Malech, H.L., Root, R.K., and Gallin, J.I. (1977). Structural analysis of human neutrophil migration: centriole, microtubule, and microfilament orientation and function during chemotaxis. J. Cell Biol. *75*, 666–693.

McGraw, T.E., Dunn, K.W., and Maxfield, F.R. (1993). Isolation of a temperature-sensitive variant Chinese hamster ovary cell line with a morphologically altered endocytic recycling compartment. J. Cell Physiol. *155*, 579–594.

Mikhailov, A., and Gundersen, G.G. (1998). Relationship between microtubule dynamics and lamellipodium formation revealed by direct imaging of microtubules in cells treated with nocodazole or taxol. Cell Motil. Cytoskeleton *41*, 325–340.

Mitchison, T.J., and Cramer, L.P. (1996). Actin-based cell motility and cell locomotion. Cell *84*, 371–379.

Otey, C., Kalnoski, M., Lessard, J., and Bulinski, J. (1986). Immunolocalization of the gamma isoform of nonmuscle actin in cultured cells. J. Cell Biol. *102*, 1726–1737.

Pierini, L.M., Lawson, M.A., Eddy, R.J., Hendey, B., and Maxfield, F.R. (2000). Oriented endocytic recycling of $\alpha5/\beta1$ in motile neutrophils. Blood *95*, 2471–2481.

Pryzwansky, K.B., and Merricks, E.P. (1998). Chemotactic peptide-induced changes of intermediate filament organization in neutrophils during granule secretion: role of cyclic guanosine monophosphate. Mol. Biol. Cell *9*, 2933–2947.

Ramsey, W.S., and Harris, A. (1973). Leukocyte locomotion and its inhibition by antimitotic drugs. Exp. Cell Res. *82*, 262–270.

Ratner, S., Sherrod, W.S., and Lichlyter, D. (1997). Microtubule retraction into the uropod and its role in T cell polarization and motility. J. Immunol. *159*, 1063–1067.

Rich, A.M., and Hoffstein, S.T. (1981). Inverse correlation between neutrophil microtubule numbers and enhanced random migration. J. Cell Sci. *48*, 181–191.

Sanchez-Madrid, F., and del Pozo, M.A. (1999). Leukocyte polarization in cell migration and immune interactions. EMBO J. *18*, 501–511.

Seveau, S., Eddy, R.J., Maxfield, F.R., and Pierini, L.M. (2001). Cytoskeleton-dependent membrane domain segregation during neutrophil polarization. Mol. Biol. Cell *12*, 3550–3562.

Seveau, S., Lopez, S., Lesavre, P., Guichard, J., Cramer, E.M., and Halbwachs-Mecarelli, L. (1997). Leukosialin (CD43, sialophorin) redistribution in uropods of polarized neutrophils is induced by CD43 cross-linking by antibodies, by colchicine or by chemotactic peptides. J. Cell Sci. *110*, 1465–1475.

Small, J.V., Rottner, K., and Kaverina, I. (1999). Functional design in the actin cytoskeleton. Curr. Opin. Cell Biol. *11*, 54–60.

Stevenson, R.D., Gray, A.C., and Lucie, N.P. (1978). Stimulation of capillary tube polymorph migration: an indirect glucocorticoid effect on microtubular function. Clin. Exp. Immunol. *33*, 478–485.

Vale, R.D. (1987). Intracellular transport using microtubule-based motors. Annu. Rev. Cell Biol. *3*, 347–378.

Waterman-Storer, C., and Salmon, E.D. (1997). Actomyosin-based retrograde flow in the lamella of migrating epithelial cells influences microtubule dynamic instability and turnover and is associated with microtubule breakage and treadmilling. J. Cell Biol. *139*, 417–434.

Wittmann, T., and Waterman-Storer, C. (2001). Cell motility. can Rho GTPases and microtubules point the way? J. Cell Sci. *114*, 3795–3808.

Yvon, A.-M.C., and Wadsworth, P. (1997). Non-centrosomal microtubule formation and measurement of minus end microtubule dynamics in A498 cells. J. Cell Sci. *110*, 2391–2401.

Zigmond, S.H. (1977). Ability of polymorphonuclear leukocytes to orient in gradients of chemotactic factors. J. Cell Biol. *75*, 606–616.

Zigmond, S.H., Levitsky, H.I., and Kreel, B.J. (1981). Cell polarity: an examination of its behavioral expression and its consequences for polymorphonuclear leukocyte chemotaxis. J. Cell Biol. *89*, 585–592.